BJR

https://doi.org/10.1259/bjr.20170470

Received: 23 June 2017 | Revised: 28 August 2017 | Accepted: 30 August 2017

Cite this article as:
Lee SH, Chang JM, Shin SU, Chu AJ, Yi A, Cho N, et al. Imaging features of breast cancers on digital breast tomosynthesis according to molecular subtype: association with breast cancer detection. *Br J Radiol* 2017; **90**: 20170470.

FULL PAPER

Imaging features of breast cancers on digital breast tomosynthesis according to molecular subtype: association with breast cancer detection

[1]SU HYUN LEE, MD, [1]JUNG MIN CHANG, MD, [1]SUNG UI SHIN, MD, [2]A JUNG CHU, MD, [3]ANN YI, MD, [1]NARIYA CHO, MD and [1]WOO KYUNG MOON, MD

[1]Department of Radiology, Seoul National University Hospital, Seoul National University College of Medicine, Seoul, Korea,
[2]Department of Radiology, Seoul Metropolitan Government-Seoul National University Boramae Medical Center, Seoul, Korea
[3]Department of Radiology, Seoul National University Hospital Healthcare System Gangnam Center, Seoul, Korea,

Address correspondence to: Prof. Jung Min Chang
E-mail: *imchangjm@gmail.com*

Objective: To evaluate imaging features of breast cancers on digital breast tomosynthesis (DBT) according to molecular subtype and to determine whether the molecular subtype affects breast cancer detection on DBT.
Methods: This was an institutional review board-approved study with a waiver of informed consent. DBT findings of 288 invasive breast cancers were reviewed according to Breast Imaging Reporting and Data System lexicon. Detectability of breast cancer was quantified by the number of readers (0–3) who correctly detected the cancer in an independent blinded review. DBT features and the cancer detectability score according to molecular subtype were compared using Fisher's exact test and analysis of variance.
Results: Of 288 invasive cancers, 194 were hormone receptor (HR)-positive, 48 were human epidermal growth factor receptor 2 (HER2) positive and 46 were triple negative breast cancers. The most common DBT findings were irregular spiculated masses for HR-positive cancer, fine pleomorphic or linear branching calcifications for HER2 positive cancer and irregular masses with circumscribed margins for triple negative breast cancers ($p < 0.001$). Cancer detectability on DBT was not significantly different according to molecular subtype ($p = 0.213$) but rather affected by tumour size, breast density and presence of mass or calcifications.
Conclusion: Breast cancers showed different imaging features according to molecular subtype; however, it did not affect the cancer detectability on DBT.
Advances in knowledge: DBT showed characteristic imaging features of breast cancers according to molecular subtype. However, cancer detectability on DBT was not affected by molecular subtype of breast cancers.

INTRODUCTION

Digital breast tomosynthesis (DBT) has been reported to increase cancer detection rates in screening when added to digital mammography (DM) because of the improved conspicuity of lesions.[1–7] However, DBT still misses a substantial number of breast cancer cases that are identified by ultrasound or magnetic resonance imaging.[8–12] According to a recent study, 72% of breast cancers missed by DBT were truly occult; the other 28% were seen retrospectively and included cancers with subtle findings and cancers that were missed due to interpretative errors.[9] Another study had reported that occult breast cancers on DBT are mainly small, infiltrating, non-calcified, non-spiculated and within dense parenchyma.[10] Although DBT can improve sensitivity compared to DM by reducing the obscuring effect of overlapping breast tissue, it remains an anatomical study without the physiological information. It is also limited in the detection of small non-calcified masses embedded in dense parenchyma without associated architectural distortion.

Breast cancers present with different mammographic features on DM according to molecular subtype. Estrogen receptor (ER) and/or progesterone receptor (PR) positive cancers tend to present as masses with irregular shape and spiculated margin; human epidermal growth factor receptor 2 (HER2) positive cancers are more likely to be associated with calcifications with fine pleomorphic or linear branching morphology; triple negative (ER, PR and HER2 negative) breast cancers are more likely to present as non-calcified masses with a relatively circumscribed margin.[13–19] On DBT, a series of thin section images of the breast are displayed. Thus, the margins of breast lesions are more conspicuous, which allows for better detection and

characterization of lesions. To the best of our knowledge, there have been no studies evaluating imaging features of breast cancers on DBT according to molecular subtype. We hypothesized that different mammographic features of breast cancers according to molecular subtype would be more apparent on DBT, and it may have effects on breast cancer detection on DBT.

Therefore, the purpose of our study was to evaluate imaging features of breast cancers on DBT according to molecular subtype and to determine whether the molecular subtype affects breast cancer detection on DBT.

METHODS AND MATERIALS

Study population

This retrospective study was approved by our institutional review board, and the requirement for written informed consent was waived. Patients who were diagnosed with invasive breast cancer and underwent DM and DBT for preoperative evaluation between December 2011 and February 2014 were included. Microinvasive breast cancer with invasive focus measuring <1 mm was not included in this study. All patients had the immunohistochemical (IHC) biomarker data for ER, PR and HER2 from surgical specimens. Of the 423 consecutive females identified in our database, 138 females were excluded because: neoadjuvant chemotherapy was administered before DBT in 44 females; vacuum-assisted core needle biopsy or surgical excision was performed before DBT in 41 females; data regarding HER2 status was incomplete in 30 females; and DBT images were unavailable in 23 females. Thus, 285 females with 288 invasive breast cancers comprised our study population.

Image acquisition

Mammography and tomosynthesis images were acquired using a commercial DM unit with tomosynthesis capability (Selenia Dimensions; Hologic, Bedford, MA,). Bilateral craniocaudal (CC) and mediolateral oblique (MLO) view images were acquired in the combo mode; DBT images were obtained along with DM images at the same breast compression. After DM acquisition, the X-ray tube and detector moved continuously over a 15° arc and acquired 15 source projection images that were reconstructed into three-dimensional DBT images, spaced in 1 mm increments, using a filtered back-projection technique. Acquisition time was approximately 10 s per view. Mean average glandular dose for a single-view DM and DBT were 1.63 and 1.74 mGy, respectively.

Image review

The review study consisted of two parts. To assess the detectability of cancers, three breast radiologists (SHL, SUS and JMC), each with 3–5 years of experience in DBT and 3–10 years of experience in DM, participated in the independent blinded review of DBT images combined with DM. The 285 study cases were randomly ordered and mixed with 62 cases of BI-RADS final assessment categories 1 or 2. A total of 347 image sets consisting of bilateral CC and MLO views were reviewed using the same workstation (SecurView; Hologic) with a 5-megapixel display monitor calibrated to the DICOM greyscale standard display function under the lowered room lights. Readers were able to pan, zoom and alter the window level of the images and marked suspicious lesions using BI-RADS final assessment.[20] When the readers detected multiple lesions in the same patient, they documented all lesions with the location of each lesion. Detectability score was assigned according to the number of readers (0–3) who correctly detected the cancer in the independent blinded review.

After that, two breast radiologists (SHL and JMC), with 6 and 10 years of experience in breast imaging, respectively, performed an unblinded review to establish reference DBT findings of the study cases. All DBT images were interpreted with knowledge of DM findings. Agreement on the lesion location, visibility and morphology of the cancers on DBT was by consensus. The two radiologists had information about operation records and pathological results except for IHC. A lesion was classified as visible if it was seen on at least one view on DBT. It was classified as non-visible if it was not seen on both CC and MLO views on DBT but detectable by ultrasound or magnetic resonance imaging. For visible lesions, findings on combined DBT and DM were described as mass only, mass with calcifications, calcifications only, focal asymmetry, or architectural distortion. Masses were evaluated for shape and margin; the morphology of calcifications were described according to the Breast Imaging Reporting and Data System (BI-RADS) lexicon.[20]

Data collection

All clinicopathological data were obtained from our prospectively maintained electronic medical record database. The clinical data collected included the patients' age at diagnosis, presence or absence of palpable symptoms, and family history of breast cancer in first-degree relatives. Pathological data collected included the histological type of breast cancer, invasive tumour size, histological grade according to the Nottingham Grading System,[21] presence or absence of carcinoma *in situ* components, lymphovascular invasion and axillary lymph node metastasis. IHC staining was performed for hormone receptor (HR) (ER and PR), HER2 and Ki-67 as part of the routine pathological assessment at our institution using standard methods.[22–24] Positivity of ER or PR was defined as nuclear staining in ≥1% of tumour cells. HER2 positivity was defined as 3+ staining at IHC or amplification of HER2 gene at fluorescence *in situ* hybridization. All of the study cases were classified into the three major subtypes using HR and HER2 status: HR+ (*i.e.* ER or PR positive and HER2 negative), HER2+ (*i.e.* ER and PR may be positive or negative) and TNBC (*i.e.* ER, PR and HER2 negative).

Statistical analysis

Clinicopathological characteristics and DBT imaging features of invasive breast cancers were compared according to molecular subtype using the Fisher's exact test for categorical variables and the analysis of variance for continuous variables. For statistical analysis, breast density was dichotomized as non-dense (BI-RADS density categories a and b) *vs* dense (BI-RADS density categories c and d). Clinicopathological and imaging factors associated with the cancer detectability score on DBT

were evaluated using ANOVA or independent samples *t*-test. Multiple linear regression analysis was performed to determine the variables independently associated with the cancer detectability score on DBT. Two-tailed *p* values of less than 0.05 indicated a statistically significant difference. All statistical analyses were performed using SPSS software (PASW Statistics, version 20; SPSS, Chicago, IL).

RESULTS

Clinicopathological factors according to molecular subtype

Of 288 cancers in 285 patients, 194 (67%) were HR+ cancer, 48 (17%) were HER2+ cancer and 46 (16%) were TNBC. Among the three patients with bilateral cancers, one had bilateral HR+ cancer and another had bilateral TNBC. The other patient had HR+ cancer in the left breast and TNBC in the right breast.

The median ages of patients with HR+, HER2+ and TNBC were 48, 52 and 52 years, respectively (p = 0.190) (Table 1). HER2+ cancer and TNBC manifested as palpable lumps more frequently (81.2 and 80.4%, respectively) than HR+ cancer (65.5%) (p = 0.027). The majority of HR+, HER2+ and TNBC had a histological type of ductal carcinoma, not otherwise specified in 82.0, 100 and 89.1%, respectively (p = 0.004). Multifocality was more frequent in HR+ and HER2+ cancers than in TNBC (p = 0.006). The median tumour sizes were 2.0, 2.1 and 2.2 cm for patients with HR-positive, HER2-positive and TNBC, respectively (p = 0.639). High histological grade and high Ki-67 index were more frequently noted in HER2+ cancer and TNBC than in HR+ cancer (p < 0.001, both). A significantly higher percentage of lymphovascular invasion was noted in HER2+ cancers (47.9%) than in HR+ cancer (25.8%) and TNBC (17.4%) (p = 0.002).

DBT imaging features of invasive breast cancers according to molecular subtype

Breast density was dense (BI-RADS density categories c and d) in 81.0, 77.0 and 73.9% of patients with HR+, HER2+ and TNBC, respectively (p = 0.532) (Table 2). DBT findings of invasive breast cancers were significantly different according to molecular subtype (p < 0.001). None of the HER2+ cancers were occult on DBT. 9 HR+ cancers (mean tumour size, 1.3 ± 0.6 cm; range, 0.5–2.5 cm; histological Grade 2 in 8 cancers and Grade 1 in one cancer) (Figure 1) and 2 TNBC (1.5 cm and histological Grade 3, both) were not visible on DBT due to small size (n = 2; 0.5 and 0.6 cm, respectively) or overlapping breast tissue (n = 9). The most frequent DBT finding was mass in HR+ [55.2% (107 of 194)] cancers (Figure 2) and TNBC [45.7% (21 of 46)] (Figure 3) followed by mass with calcifications [29.4% (57 of 194) and 39.1% (18 of 46) for HR+ and TNBC, respectively]. In contrast, HER2+ cancers appeared as mass with calcifications most frequently [54.2% (26 of 48)] followed by calcifications only [25.0% (12 of 48)] (Figure 4). The frequency of cancers presenting as masses on DBT was not significantly different between HR+, HER2+ and TNBC [84.5% (164 of 194), 72.9% (35 of 48) and 84.8% (39 of 46), respectively] (p = 0.150). However, the morphology of masses was different according to molecular subtype. An irregular mass with circumscribed margin was the most frequent feature in TNBC. However, TNBCs were more frequently oval or round in shape [46.1% (18 of 39)] than HER2+ [25.7% (9 of 35)] and HR+ [12.8% (21 of 164)] cancers (p< 0.001). TNBCs were also less likely to have spiculated margins [23.1% (9 of 39)] than HER2+ [34.3% (12 of 35)] and HR+ [56.1% (92 of 164)] cancers (p < 0.001). As for the calcifications, a significantly higher percentage of HER2+ cancer [79.2% (38 of 48)] presented as calcifications on DBT than HR+ cancer [35.1% (68 of 194)] and TNBC [47.8% (22 of 46)] (p < 0.001). Calcifications associated with HER2+ cancer were more frequently fine linear and linear branching in morphology than HR+ and TNBC (p < 0.001).

Factors associated with cancer detectability on DBT

The cancer detectability score, determined by the number of readers who correctly detected the cancer on DBT, was 2.74 ± 0.69 [mean ± standard deviation (SD)] overall, 2.70 ± 0.74 for HR+ cancer, 2.89 ± 0.31 for HER2+ cancer and 2.74 ± 0.71 for TNBC (Table 3). 11 non-visible cancers (9 HR+ cancers and 2 TNBC) were not detectable by any readers. The mean cancer detectability score of HER2+ cancer was slightly higher than that of HR+ or TNBC; however, this difference was not statistically significant (p = 0.213). Among the other clinicopathological factors, higher cancer detectability score was significantly associated with age ≥50 years (p = 0.010), larger invasive tumour size (p < 0.001) and higher histological grade (p = 0.023). The mean cancer detectability score was not significantly different according to the histological type of cancers (p = 0.496). Cancer detectability was significantly higher in non-dense breast than in dense breast (p = 0.001) (Table 4). Cancer detectability was significantly different according to the lesion type on DBT (p = 0.001). Presence of mass or calcification was associated with higher detectability score (p < 0.001, both). Indistinct margin of mass was associated with lower detectability (p = 0.002). However, mass shape or morphology of calcification was not associated with cancer detectability (p > 0.50). Variables that showed statistical significance (p < 0.05) on univariate analysis were included in the multivariate analysis. In multivariate analysis, larger invasive tumour size (p = 0.006), non-dense breast density (p = 0.029), presence of mass on DBT (p < 0.001) and presence of calcification on DBT (p < 0.001) were significant independent factors associated with higher cancer detectability score.

DISCUSSION

DBT is being increasingly used for breast cancer screening as well as diagnostic evaluation in addition to DM, leading to better detection and characterization of breast lesions. Clinical evidence suggests that mammographic findings and histopathological prognostic markers including molecular subtype are correlated in breast cancers.[13–18] To our knowledge, DBT features of breast cancers according to molecular subtype have not been previously reported. So far, increased cancer detection by adding DBT to DM was mainly reported in screening population. In those previous studies, it was described that

Table 1. Clinical and histological features of 288 invasive breast cancers according to molecular subtype

	Total (n = 288)	Molecular subtype			p-value
		HR+ (n = 194)	HER2+ (n = 48)	TNBC (n = 46)	
Age (years)					0.190
Mean (SD)	50.8 (10.6)	50.0 (10.1)	52.5 (11.1)	52.4 (11.9)	
Median (range)	49 (22–78)	48 (22–77)	52 (30–73)	52 (30–78)	
Clinical manifestation					0.027
Asymptomatic	85 (29.5)	67 (34.5)	9 (18.8)	9 (19.6)	
Palpable lump	203 (70.5)	127 (65.5)	39 (81.2)	37 (80.4)	
FHx of breast cancer					0.793
Absent	272 (94.4)	184 (94.8)	45 (93.8)	43 (93.5)	
Present	16 (5.6)	10 (5.2)	3 (6.3)	3 (6.5)	
Histological type					0.004
Ductal, NOS	248 (86.1)	159 (82.0)	48 (100)	41 (89.1)	
Dctal, special	18 (6.3)	14 (7.2)	0 (0)	4 (8.7)	
Lbular	22 (7.6)	21 (10.8)	0 (0)	1 (2.2)	
Focality					0.006
Unifocal	205 (71.2)	135 (69.6)	29 (60.4)	41 (89.1)	
Multifocal	83 (28.8)	59 (30.4)	19 (39.6)	5 (10.9)	
Tumour size (cm)					0.639
Mean (SD)	2.3 (1.3)	2.2 (1.3)	2.2 (1.1)	2.4 (1.2)	
Median (range)	2.0 (0.1–9.5)	2.0 (0.1–9.5)	2.1 (0.2–5.3)	2.2 (0.4–7.7)	
Histological grade					<0.001
1 or 2	138 (47.9)	127 (65.5)	5 (10.4)	6 (13.0)	
3	150 (52.1)	67 (34.5)	43 (89.6)	40 (87.0)	
Associated DCIS					0.087
Absent	57 (19.8)	42 (21.6)	4 (8.3)	11 (23.9)	
Present	231 (80.2)	152 (78.4)	44 (91.7)	35 (76.1)	
Lymphovascular invasion					0.002
Absent	207 (71.9)	144 (74.2)	25 (52.1)	38 (82.6)	
Present	81 (28.1)	50 (25.8)	23 (47.9)	8 (17.4)	
Axillary lymph node metastasis					0.159
Absent	203 (70.5)	136 (70.1)	30 (62.5)	37 (80.4)	
Present	85 (29.5)	58 (29.9)	18 (37.5)	9 (19.6)	
Ki-67 index					<0.001
Low (<14%)	236 (81.9)	183 (94.3)	31 (64.6)	22 (47.8)	
High (≥14%)	52 (18.1)	11 (5.7)	17 (35.4)	24 (52.2)	

Note. DCIS, ductal carcinoma *in situ*; FHx, family history; HER2+, human epidermal growth factor receptor 2; HR+, hormone receptor; NOS, not otherwise specified; SD, standard deviation; TNBC, triple negative breast cancer. Data are numbers of cancers with percentages in parentheses unless otherwise indicated.

additional benefit was noted in invasive cancers; however, their molecular subtype was not described.[1–7] In this study, we evaluated imaging features of breast cancers on DBT according to molecular subtype and their effects on cancer detectability on DBT. Our results showed that invasive breast cancers presented with different imaging features on DBT according to molecular subtype ($p < 0.001$) although it did not affect cancer detectability.

Table 2. Imaging features of 288 invasive breast cancers on digital breast tomosynthesis according to molecular subtype

	HR+ (n = 194)	HER2+ (n = 48)	TNBC (n = 46)	p-value
Breast density				0.923
a	8 (4.1)	2 (4.2)	3 (6.5)	
b	29 (14.9)	9 (18.8)	9 (19.6)	
c	114 (58.8)	27 (56.2)	26 (56.5)	
d	43 (22.2)	10 (20.8)	8 (17.4)	
a-b (non-dense)	37 (19.0)	11 (23.0)	12 (26.1)	0.532
c-d (dense)	157 (81.0)	37 (77.0)	34 (73.9)	
Lesion type on DBT				<0.001
Negative (not visible)	9 (4.6)	0 (0)	2 (4.3)	
Focal asymmetry	6 (3.1)	1 (2.1)	1 (2.2)	
Calcifications only	11 (5.7)	12 (25.0)	4 (8.7)	
Mass only	110 (56.7)	9 (18.8)	21 (45.7)	
Mass with calcifications	58 (29.9)	26 (54.2)	18 (39.1)	
Presence of mass				0.068
Yes	168 (86.6)	35 (72.9)	39 (84.8)	
No	26 (13.4)	13 (27.1)	7 (15.2)	
Mass shape[a]				<0.001
Oval	10 (6.0)	4 (11.4)	10 (25.6)	
Round	11 (6.5)	5 (14.3)	8 (20.5)	
Irregular	147 (87.5)	26 (74.3)	21 (53.8)	
Mass margin[a]				<0.001
Circumscribed	18 (10.7)	4 (11.4)	13 (33.3)	
Obscured	4 (2.4)	1 (2.9)	4 (10.3)	
Microlobulared	18 (10.7)	8 (22.9)	7 (17.9)	
Indistinct	32 (19.0)	10 (28.6)	6 (15.4)	
Spiculated	96 (57.1)	12 (34.3)	9 (23.1)	
Presence of calcifications				<0.001
Yes	68 (35.1)	38 (79.2)	22 (47.8)	
No	126 (64.9)	10 (20.8)	24 (52.2)	
Calcification morphology[b]				<0.001
Amorphous	35 (51.5)	8 (21.1)	14 (63.6)	
Coarse heterogeneous	9 (13.2)	2 (5.3)	0 (0)	
Fine pleomorphic	21 (30.9)	17 (44.7)	7 (31.8)	
Fine linear or linear branching	3 (4.4)	11 (28.9)	1 (4.5)	

Note. DBT, digital breast tomosynthesis; HR, hormone receptor; HER2, human epidermal growth factor receptor 2; TNBC, triple negative breast cancer. Data are numbers of cancers with percentages in parentheses.

[a]Percentages were calculated with a denominator of 168 in HR+ cancer, 35 in HER2+ cancer and 39 in TNBC.

[b]Percentages were calculated with a denominator of 68 in HR+ cancer, 38 in HER2 + cancer and 22 in TNBC.

The most characteristic findings of breast cancers on DBT according to molecular subtype were an irregular spiculated mass for HR+ cancer, fine pleomorphic or fine linear branching calcifications with or without a mass for HER2+ cancer and an oval or round mass with circumscribed margin for TNBC. Previous studies have reported that TNBC frequently presented as a mass with round shape and non-spiculated margin on DM.[14,15,25–28] In contrast, HR+ and HER2+ cancers are known to exhibit typical

Figure 1. Images in a 40-year-old female with a 0.5 cm, HR positive, histological Grade 2, invasive ductal carcinoma in dense breast (grade d). Mediolateral oblique DM (a) and DBT (b) images show negative findings. None of the readers detected the cancer on DBT in combination with DM (detectability score 0). (c) Ultrasound depicted a round indistinct hypoechoic mass in the left breast at 6 o'clock location. (d) Mediolateral oblique DM obtained after ultrasound-guided hook-wire localization is also negative for cancer. DBT, digital breast tomosynthesis; DM, digital mammography.

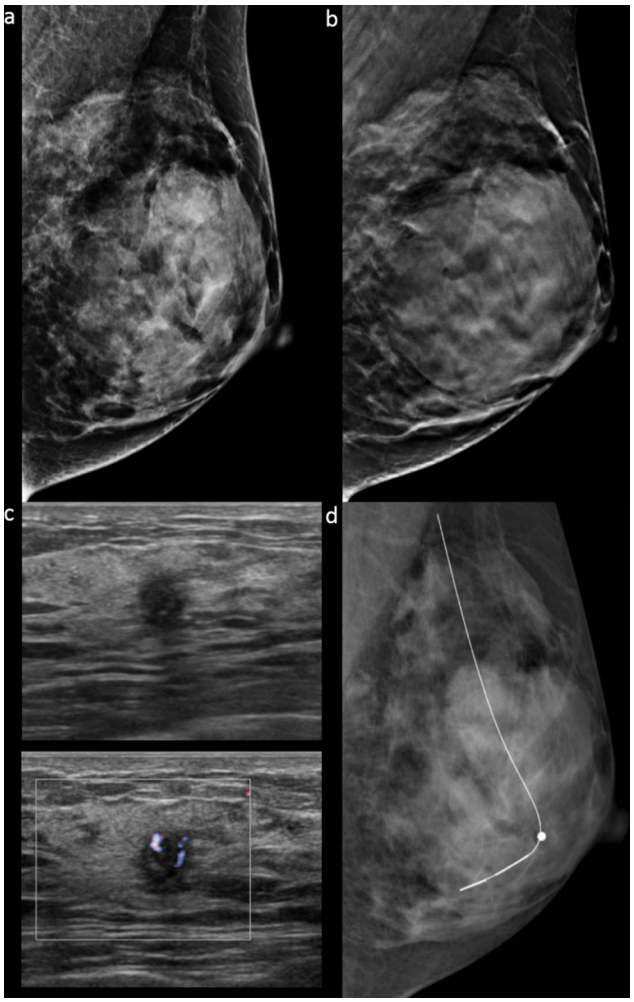

breast cancer findings of masses with irregular shape and spiculated margins for HR+ cancers and fine pleomorphic or fine linear branching calcifications for HER2+ cancers on DM, similar to our study results using DBT.[14,17,19,25]

The strength of our study is that the cancer detectability on DBT was quantified by the numbers of radiologists who correctly detected the cancer, and its association with various clinical, imaging and pathological factors was evaluated. Our study showed that DBT led to higher detectability for cancers with larger invasive tumour size presenting as a mass or calcifications in non-dense breast. Although DBT findings of breast cancers were significantly different according to molecular subtype, DBT in combination with DM had similar detectability for

Figure 2. Images in a 40-year-old female with a 2.3 cm, HR positive, histological Grade 3, invasive ductal carcinoma in dense breast (grade c). Craniocaudal DM (a) and DBT (b) images show a mass with irregular shape and spiculated margin in the right inner breast that was detected by all three readers (detectability score 3).

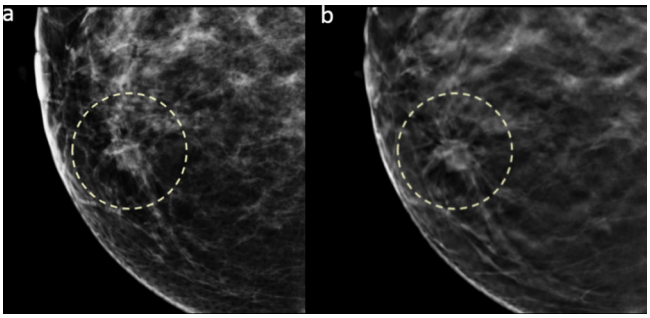

Figure 4. Images in a 56-year-old female with a 1.5 cm, HER2 positive, histological Grade 3, invasive ductal carcinoma in dense breast (grade d). Craniocaudal DM (a) and DBT (b) images show grouped fine pleomorphic calcifications in the left outer breast that were detected by all three readers (detectability score 3).

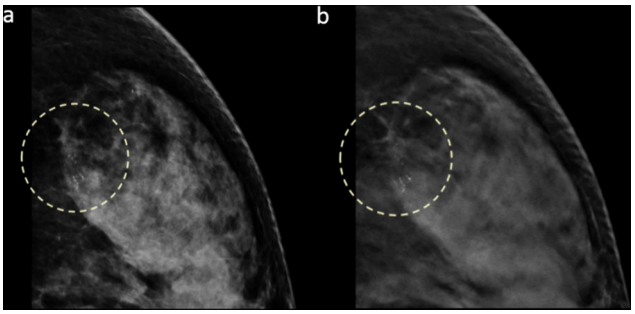

cancers with different subtypes. HER2+ cancer had a slightly higher detectability score than HR+ cancer and TNBC; none of the HER2+ cancers were occult on DBT. The higher detectability of HER2+ cancers on DBT could be owing to the higher frequency of cases presenting with calcifications.[29] However, this

Figure 3. Images in a 64-year-old female with a 2.0 cm, triple negative, histological Grade 3, invasive ductal carcinoma in dense breast (grade c). Craniocaudal DM (a) and DBT (b) images show a mass with oval shape and circumscribed margin in the left breast subareolar region that was detected by all three readers (detectability score 3).

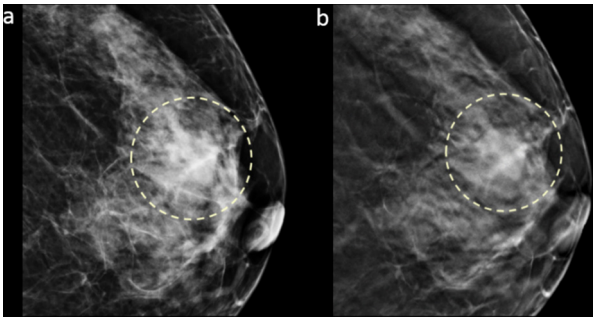

difference did not reach statistical significance. Although TNBC showed fewer typical features of malignancy than HR+ cancer, most readers correctly assessed TNBC on DBT as suspicious for malignancy and needed to be biopsied.

In our study, histological type was not a significant factor associated with cancer detectability on DBT. It has been reported that invasive lobular carcinoma is difficult to detect on DM because it typically comprises small bland cells that infiltrate along and around ducts in a single file without destroying the underlying architecture.[30] In our study, DBT showed comparable detectability scores for both ductal and lobular cancers. Our results are similar to those of a recent study reporting that adding DBT to DM significantly improved identification and interpretive accuracy of mammographic interpretation for invasive lobular carcinoma cases.[31] Although DBT can improve cancer detection and characterization by reducing tissue overlap, DBT still has a limitation in detecting small, non-calcified invasive cancers or cancers with subtle findings in dense breasts. Additional imaging such as ultrasound may be needed to detect early cancers in females with dense breasts and negative findings on DBT.

There are limitations to our study. First, this was a retrospective study with a relatively small sample size. Further investigation in a larger study population is warranted. Second, only three readers were involved in the blinded reader study. In addition, two of the three readers participated in the next unblinded review and this could have biased the results. Third, we did not assess the probability of malignancy for each lesion based on final BI-RADS assessment categories or percentage scale. Our study was aimed at evaluating cancer detection on DBT; therefore, readers assessed for lesions suspicious for malignancy regardless of the probability for malignancy. Fourth, our study was conducted in cancer-enriched population to assess cancer detectability and morphological characteristics using DBT information. Therefore, the results

Table 3. Cancer detectability score on digital breast tomosynthesis according to clinical and pathological factors

Parameter	No. of cancers	Cancer detectability score	
		Mean ± SD	*p*-value
Age (years)			0.010
<50	151	2.64 ± 0.79	
≥50	137	2.85 ± 0.53	
Palpable symptom			0.082
Absent	85	2.62 ± 0.75	
Present	203	2.79 ± 0.65	
Invasive tumour size			<0.001
≤1 cm	39	2.26 ± 1.07	
1–2 cm	111	2.69 ± 0.74	
>2 cm	138	2.91 ± 0.37	
Histological type			0.496
Ductal, NOS	248	2.75 ± 0.66	
Ductal, special type	18	2.55 ± 0.98	
Lobular	22	2.73 ± 0.70	
Presence of DCIS			0.298
Absent	57	2.82 ± 0.60	
Present	231	2.72 ± 0.71	
Histological grade			0.023
1	11	2.45 ± 1.03	
2	127	2.64 ± 0.81	
3	150	2.84 ± 0.51	
Molecular subtype			0.213
HR+	194	2.70 ± 0.74	
HER2+	48	2.89 ± 0.31	
TNBC	46	2.74 ± 0.71	

Note. DCIS, ductal carcinoma *in situ*; HR+, hormone receptor; HER2+, human epidermal growth factor receptor 2; NOS, not otherwise specified; SD, standard deviation; TNBC, triple negative breast cancer.

Table 4. Cancer detectability score on digital breast tomosynthesis according to imaging factors

Parameter	No. of cancers	Cancer detectability score	
		Mean ± SD	*p*-value
Breast density			0.001
Non-dense	60	2.93 ± 0.41	
Dense	228	2.69 ± 0.73	
Lesion type on DBT			<0.001
Negative (not visible)	11	0.00	
Focal asymmetry	8	2.00 ± 0.92	
Calcifications only	27	2.74 ± 0.53	
Mass only	140	2.84 ± 0.40	
Mass with calcifications	102	2.95 ± 0.26	
Presence of mass			<0.001
Yes	242	2.89 ± 0.35	
No	46	1.96 ± 1.26	
Mass shape			0.517
Oval	24	2.92 ± 0.41	
Round	24	2.96 ± 0.20	
Irregular	194	2.88 ± 0.36	
Mass margin			0.002
Circumscribed	35	2.97 ± 0.17	
Obscured	9	3.00 ± 0.00	
Microlobulated	33	2.88 ± 0.33	
Indistinct	48	2.71 ± 0.54	
Spiculated	117	2.93 ± 0.29	
Presence of calcifications			<0.001
Yes	128	2.91 ± 0.34	
No	160	2.61 ± 0.85	
Calcification morphology			0.593
Amorphous	57	2.89 ± 0.41	
Coarse heterogeneous	11	2.82 ± 0.40	
Fine pleomorphic	45	2.91 ± 0.29	
Fine linear or linear branching	15	3.00 ± 0.00	

DBT, digital breast tomosynthesis; SD, standard deviation.

might not be directly applicable to the screening population. Further study in screening populations is warranted. Lastly, we did not evaluate comparative detectability scores between DM and DBT. More studies comparing the detectability of cancers on DM and DBT according to molecular subtype are warranted for the next step to prove the additional benefit of DBT in each subtype.

In conclusion, breast cancers have different imaging findings on DBT according to molecular subtype. However, the subtype of breast cancer was not a significant factor in determining the cancer detectability on DBT. Instead, the detectability of breast cancers on DBT was affected by invasive tumour size, breast density and presence of mass or calcifications on DBT. These findings will need further validation in larger studies.

FUNDING

This research was supported by a grant of the Korea Health Technology R&D Project through the Korea Health Industry Development Institute (KHIDI), funded by the Ministry of Health and Welfare, Republic of Korea (grant number: HI15C1532).

REFERENCES

1. Ciatto S, Houssami N, Bernardi D, Caumo F, Pellegrini M, Brunelli S, et al. Integration of 3D digital mammography with tomosynthesis for population breast-cancer screening (STORM): a prospective comparison study. *Lancet Oncol* 2013; **14**: 583–589. doi: https://doi.org/10.1016/S1470-2045(13)70134-7
2. Skaane P, Bandos AI, Gullien R, Eben EB, Ekseth U, Haakenaasen U, et al. Comparison of digital mammography alone and digital mammography plus tomosynthesis in a population-based screening program. *Radiology* 2013; **267**: 47–56. doi: https://doi.org/10.1148/radiol.12121373
3. Friedewald SM, Rafferty EA, Rose SL, Durand MA, Plecha DM, Greenberg JS, et al. Breast cancer screening using tomosynthesis in combination with digital mammography. *JAMA* 2014; **311**: 2499–507. doi: https://doi.org/10.1001/jama.2014.6095
4. McCarthy AM, Kontos D, Synnestvedt M, Tan KS, Heitjan DF, Schnall M, et al. Screening outcomes following implementation of digital breast tomosynthesis in a general-population screening program. *J Natl Cancer Inst* 2014; **106**. doi: https://doi.org/10.1093/jnci/dju316
5. Korporaal JG, Mertelmeier T. Comparison of digital breast tomosynthesis and two-dimensional mammography. *Radiology* 2016; **280**: 980–981. doi: https://doi.org/10.1148/radiol.2016160321
6. Rafferty EA, Durand MA, Conant EF, Copit DS, Friedewald SM, Plecha DM, et al. Breast cancer screening using tomosynthesis and digital mammography in dense and nondense breasts. *JAMA* 2016; **315**: 1784–1786. doi: https://doi.org/10.1001/jama.2016.1708
7. Sharpe RE, Jr, Venkataraman S, Phillips J, Dialani V, Fein-Zachary VJ, Prakash S, et al. Increased cancer detection rate and variations in the recall rate resulting from implementation of 3D digital breast tomosynthesis into a population-based screening program. *Radiology* 2016; **278**: 698–706. doi: https://doi.org/10.1148/radiol.2015142036
8. Tagliafico AS, Calabrese M, Mariscotti G, Durando M, Tosto S, Monetti F, et al. Adjunct screening with tomosynthesis or ultrasound in women with mammography-negative dense breasts: interim report of a prospective comparative trial. *J Clin Oncol* 2016; **34**: 1882–8. doi: https://doi.org/10.1200/JCO.2015.63.4147
9. Andrejeva-Wright L, Hooley R, Eng K, Weisiger J, Raghu M, Butler R. Clinical and Imaging Features of Tomosynthesis Occult Breast Cancer and Reasons for Non-Detection. Radiological Society of North America 2015 Scientific Assembly and Annual Meeting, November 29 - December 4. 2015. Available from: https://rsna2015.rsna.org/program/details/?emID=15002254 [Accessed 21 December 2016]
10. Pinochet M, Horvath E, Rochels M, Silva Fuente-Alba C, Uchida M, Duran Caro M. Missed breast cancer by digital mammography and tomosynthesis. Radiological Society of North America 2015 Scientific Assembly and Annual Meeting, November 29 - December 4. 2015. Available from: https://rsna2015.rsna.org/program/details/?emID=15002283 [Accessed 21 December 2016]
11. Korhonen KE, Weinstein SP, McDonald ES, Conant EF. Strategies to increase cancer detection: review of true-positive and false-negative results at digital breast tomosynthesis screening. *Radiographics* 2016; **36**: 1954–1965. doi: https://doi.org/10.1148/rg.2016160049
12. Kim WH, Chang JM, Moon HG, Yi A, Koo HR, Gweon HM, et al. Comparison of the diagnostic performance of digital breast tomosynthesis and magnetic resonance imaging added to digital mammography in women with known breast cancers. *Eur Radiol* 2016; **26**: 1556–1564. doi: https://doi.org/10.1007/s00330-015-3998-3
13. Luck AA, Evans AJ, James JJ, Rakha EA, Paish EC, Green AR, et al. Breast carcinoma with basal phenotype: mammographic findings. *AJR Am J Roentgenol* 2008; **191**: 346–351. doi: https://doi.org/10.2214/AJR.07.2659
14. Yang WT, Dryden M, Broglio K, Gilcrease M, Dawood S, Dempsey PJ, et al. Mammographic features of triple receptor-negative primary breast cancers in young premenopausal women. *Breast Cancer Res Treat* 2008; **111**: 405–410. doi: https://doi.org/10.1007/s10549-007-9810-6
15. Kojima Y, Tsunoda H. Mammography and ultrasound features of triple-negative breast cancer. *Breast Cancer* 2011; **18**: 146–151. doi: https://doi.org/10.1007/s12282-010-0223-8
16. Tamaki K, Ishida T, Miyashita M, Amari M, Ohuchi N, Tamaki N, et al. Correlation between mammographic findings and corresponding histopathology: potential predictors for biological characteristics of breast diseases. *Cancer Sci* 2011; **102**: 2179–85. doi: https://doi.org/10.1111/j.1349-7006.2011.02088.x
17. Killelea BK, Chagpar AB, Bishop J, Horowitz NR, Christy C, Tsangaris T, et al. Is there a correlation between breast cancer molecular subtype using receptors as surrogates and mammographic appearance? *Ann Surg Oncol* 2013; **20**: 3247–353. doi: https://doi.org/10.1245/s10434-013-3155-7
18. Radenkovic S, Konjevic G, Isakovic A, Stevanovic P, Gopcevic K, Jurisic V. HER2-positive breast cancer patients: correlation between mammographic and pathological findings. *Radiat Prot Dosimetry* 2014; **162**: 125–128. doi: https://doi.org/10.1093/rpd/ncu243
19. Cho N. Molecular subtypes and imaging phenotypes of breast cancer. *Ultrasonography* 2016; **35**: 281–288. doi: https://doi.org/10.14366/usg.16030
20. Sickles EA, D'Orsi CJ, Bassett LW, Appleton CM, Berg WA, Burnside ES. ACR BI-RADS Mammography. In: *ACR BI-RADS Atlas, Breast Imaging Reporting and Data System*. Reston, VA: American College of Radiology; 2013. pp. 13–140.
21. Elston CW, Ellis IO. Pathological prognostic factors in breast cancer. I. The value of histological grade in breast cancer: experience from a large study with long-term follow-up. *Histopathology* 2002; **41(3A)**: 154–61.
22. Hammond ME, Hayes DF, Dowsett M, Allred DC, Hagerty KL, Badve S, et al. American society of clinical oncology/College of american pathologists guideline recommendations for immunohistochemical testing of estrogen and progesterone receptors in breast cancer. *J Clin Oncol* 2010; **28**: 2784–2795. doi: https://doi.org/10.1200/JCO.2009.25.6529
23. Wolff AC, Hammond ME, Schwartz JN, Hagerty KL, Allred DC, Cote RJ, et al. American Society of Clinical Oncology/College of American Pathologists guideline recommendations for human epidermal growth factor receptor 2 testing in breast cancer. *J Clin Oncol* 2007; **25**: 118–145. doi: https://doi.org/10.1200/JCO.2006.09.2775
24. Dowsett M, Nielsen TO, A'Hern R, Bartlett J, Coombes RC, Cuzick J, et al. Assessment of Ki67 in breast cancer: recommendations from the International Ki67 in Breast cancer working group. *J Natl Cancer Inst* 2011; **103**: 1656–64. doi: https://doi.org/10.1093/jnci/djr393
25. Boisserie-Lacroix M, Macgrogan G, Debled M, Ferron S, Asad-Syed M, McKelvie-Sebileau P, et al. Triple-negative breast cancers: associations between imaging and pathological findings for triple-negative

tumors compared with hormone receptor-positive/human epidermal growth factor receptor-2-negative breast cancers. *Oncologist* 2013; **18**: 802–811. doi: https://doi.org/10.1634/theoncologist.2013-0380

26. Kim MY, Choi N. Mammographic and ultrasonographic features of triple-negative breast cancer: a comparison with other breast cancer subtypes. *Acta Radiol* 2013; **54**: 889–94. doi: https://doi.org/10.1177/0284185113488580
27. Gao B, Zhang H, Zhang SD, Cheng XY, Zheng SM, Sun YH, et al. Mammographic and clinicopathological features of triple-negative breast cancer. *Br J Radiol* 2014; **87**: 20130496. doi: https://doi.org/10.1259/bjr.20130496
28. Jung HK, Han K, Lee YJ, Moon HJ, Kim EK, Kim MJ. Mammographic and sonographic features of triple-negative invasive carcinoma of no special type. *Ultrasound Med Biol* 2015; **41**: 375–83. doi: https://doi.org/10.1016/j.ultrasmedbio.2014.09.006
29. Seo BK, Pisano ED, Kuzimak CM, Koomen M, Pavic D, Lee Y, et al. Correlation of HER-2/neu overexpression with mammography and age distribution in primary breast carcinomas. *Acad Radiol* 2006; **13**: 1211–8. doi: https://doi.org/10.1016/j.acra.2006.06.015
30. Porter AJ, Evans EB, Foxcroft LM, Simpson PT, Lakhani SR. Mammographic and ultrasound features of invasive lobular carcinoma of the breast. *J Med Imaging Radiat Oncol* 2014; **58**: 1–10. doi: https://doi.org/10.1111/1754-9485.12080
31. Mariscotti G, Durando M, Houssami N, Zuiani C, Martincich L, Londero V, et al. Digital breast tomosynthesis as an adjunct to digital mammography for detecting and characterising invasive lobular cancers: a multi-reader study. *Clin Radiol* 2016; **71**: 889–895. doi: https://doi.org/10.1016/j.crad.2016.04.004